Biochimica et Biophysica Acta, 634 (1981) 203—218

BBA 47988

CONTROL OF ENERGY TRANSFORMATION IN MITOCHONDRIA

ANALYSIS BY A QUANTITATIVE MODEL

RALF BOHNENSACK

Institut für Physiologische Chemie, Medizinische Akademie, DDR-301 Magdeburg (G.D.R.)

(Received June 17th, 1980)
(Revised manuscript received September 28th, 1980)

Key words: Oxidative phosphorylation; Computer simulation; Proton translocation; Adenine nucleotide translocation; Energy transformation

Summary

A mathematical model of control of energy transformation in mitochondria is presented. The considered processes are: the proton translocation by the respiratory chain, the production of ATP by ATPase, the translocation of adenine nucleotides and of phosphate by their translocators, and a passive backflow of protons through the mitochondrial membrane. The mathematical equations expressing the steady-state kinetics of these processes and the relations between them were derived on the basis of current experimental data. The model predicts fairly well the values of the proton electrochemical gradient, of the ATP/ADP ratios within and outside mitochondria and of the distribution of phosphate between both compartments in different metabolic states of mitochondria. From the general agreement of model computations with experimental data, it is suggested that the electron flux through the respiratory chain is immediately controlled by the energy back-pressure of the proton electrochemical gradient, that the ATPase reaction is in near equilibrium in phosphorylating mitochondria but that the adenine nucleotide exchange across the mitochondrial membrane requires some loss of energy. The latter is caused by an inhibition of the translocator by ATP from the outer side or by ADP from the inner side depending on the actual ATP/ADP in both compartments. It explains that no fixed relation exists between the rate of respiration and the phosphorylation state of extramitochondrial adenine nucleotides. The relation

---

Abbreviations and symbols: $\Delta G_{P,E}$ and $\Delta G_{P,I}$, phosphorylation potential in the extramitochondrial and intramitochondrial compartment; $\Delta\mu$, proton electrochemical gradient; $\Delta\psi$, membrane potential; $Z = 2.3\ RT/F$; P/O, number of phosphorylated molecules ADP per atom oxygen consumed in respiration.

is modified by the concentration of phosphate and by intramitochondrial energy utilization.

Introduction

Mitochondria catalyze the transfer of energy delivered during the oxidation of substrates into ATP and into ion gradients across their inner membrane. If the concentrations of substrate and of oxygen are saturating, the rate of energy transformation depends only on the energy utilization and on the capacity of the mitochondria. The control phenomena caused by the utilization of ATP outside mitochondria are experimentally well described. Within a control range, the stationary rate of oxidative phosphorylation depends on the resulting extramitochondroal ATP/ADP ratio [1—4]. The rate has its minimum in the resting state, in absence of ATP utilization, whereas its maximum occurs in the active state at low ATP/ADP ratios. Inorganic phosphate was found to change the maximum rate but to have only small effects on the control range [4—6].

In the present paper, the mechanisms which produce this behaviour are analyzed on the basis of the generally accepted chemiosmotic concept of energy transfer [7]. For this purpose, the function of energy-transforming units of mitochondria, i.e. respiratory chain, ATPase, translocators of phosphate and of adenine nucleotides, are described by mathematical equations. The equations were developed from an earlier model [8] which was not in accordance with the chemiosmotic-coupling theory. It is shown that the behaviour predicted by the resulting mathematical model is in good agreement with the experimental data. From this it is concluded that a rapid energy equilibration exists between the respiratory chain, the proton electrochemical gradient across the membrane and the intramitochondrial adenine nucleotide system. The relation to the extramitochondrial adenine nucleotide system is under kinetic control by the adenine nucleotide translocator.

Methodology

The respiratory chain, the ATPase and the translocators of adenine nucleotides and of phosphate can be considered as energy-transforming units. As depicted in Fig. 1, they convert the chemical energy, delivered by substrate oxidation, into the proton electrochemical gradient, into the intramitochondrial phosphorylation potential and, finally, into the extramitochondrial phosphorylation potential. The energy flux caused by the different processes utilizing energy, i.e. ion translocations across the mitochondrial membrane and ATP consumption within and outside mitochondria, is determined by the kinetic properties of the energy-transforming processes. The mathematical equations used here for their description and the corresponding parameters are listed in Table I. In the following, the biochemical interpretation of the selected equations and values will be given (for mathematical details see Appendices 1—4).

The complex kinetics of the respiratory chain is summarized in three reactions: the supply of hydrogen, the reversible energy transformation into the proton electrochemical gradient and the terminal oxidation. The reason for this

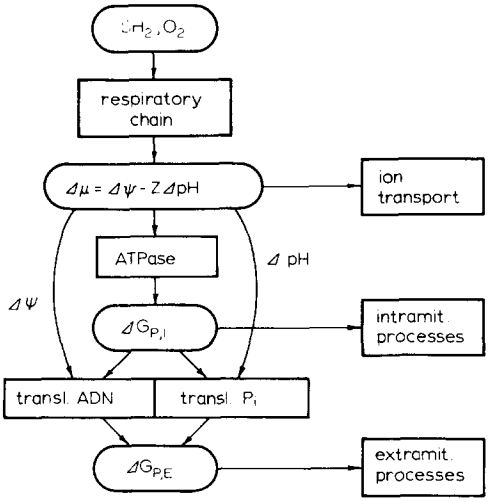

Fig. 1. Scheme of energy transforming processes in mitochondria and their connection with energy utilizing processes. ⬭, energy pool; ▭ metabolic activity; ⟶, direction of energy flux.

separation is the irreversibility of the cytochrome oxidase (even under conditions [9] which widely favour the reversed reaction) and the limitation of the maximum overall rate of respiration by the supply of hydrogen. The latter is indicated by the dependence of the respiration rate on the kind of substrate oxidized and by experiments with specific inhibitors [5,10]. This step is considered here to be irreversible, too, which is permissible if the concentration of the oxidized substrate is negligible. The kinetics of the two irreversible steps is approximated by simple first-order reactions (Eqns. 1 and 3). In the rate law of the second, the reversible reaction (Eqn. 2), the kinetic effects caused by the deviations of the mass-action ratio from the equilibrium value are the only factors taken into account. For the structure of Eqn. 2 see Appendix 1. It is shown that other kinetic effects can be neglected if a reaction is fast enough in comparison to the net flux.

The maximum velocity of the first step is arbitrarily chosen as unity to express all of the flux rates occurring in the system, therefore, $V_h = 1$. The corresponding value of the second step was taken from the information given by Wilson and coworkers [11,12] that the electron exchange within the respiratory chain is 1000-times faster than the net flux. The value of the maximum velocity of the third step determined the degree of oxidation of the terminal donator at a given respiration rate (cf. Eqn. 3). Therefore, it influences the actual potential gap between the redox systems A and D which is reversibly transformed by reaction 2 into the proton electrochemical gradient. The value $V_o = 1000$ was chosen because it gives $\Delta\mu \approx -200$ mV in the resting state, as measured in earlier experiments [13—17]. For the number of protons translocated by the three coupling sites involved in reaction 2, different values are published ranging from 2—4 $H^+/2e^-$ for each site (cf. Refs. 18—21 and the citations given there). The value $n_r = 9$ is based on thermodynamic estimations [13,14], resulting in an average of $3H^+/2e^-$ per site. The parameter $\Delta\mu_r$ is used to express the equilibrium constant of the reaction by means of the proton

TABLE I

MATHEMATICAL MODEL OF ENERGY TRANSFORMATION IN MITOCHONDRIA

The set of mathematical equations describes steady-state fluxes. The biochemical significance of the equations and the selection of the parameter values are outlined in Methodology. Abbreviations and symbols: SH_2, S, reduced and oxidized form of the substrate; A_{ox}, A_{red}, oxidized and reduced component of the respiratory chain which is reduced from the substrate side in a rate-limiting step; D_{ox}, D_{red}, oxidized and reduced form of the terminal component in the respiratory chain; a_{ox}, a_{red}, d_{ox}, d_{red}, mole fractions as $a_{ox} = [A_{ox}]/([A_{ox}] + [A_{red}])$; n_r, n_a, stoichiometric coefficients of protons translocated by the respiratory chain and by the ATPase, respectively; $\Delta\mu_r$, $\Delta\mu_a$, proton electrochemical gradients equivalent to the

No.	Equations	Parameters
	Respiratory chain	
	input of hydrogen	
	$SH_2 + A_{ox} \xrightarrow{v_h} S + A_{red}$	
1	$v_h = V_h \cdot a_{ox}$	$V_h = 1$ *
	energy transformation	
	$A_{red} + 2D_{ox} + n_r H_I^+ \overset{v_r}{\rightleftharpoons} A_{ox} + 2D_{red} + n_r H_E^+$	$n_r = 9$
2	$v_r = V_r\left(1 - \frac{a_{ox} \cdot d_{red}^2}{a_{red} \cdot d_{ox}^2} \cdot 10^{-n_r(\Delta\mu - \Delta\mu_r)/Z}\right)$	$V_r = 1000$ * $\Delta\mu_r = -150$ mV $Z = 60$ mV
	terminal oxidation	
	$2\,D_{red} + 1/2\,O_2 \xrightarrow{v_o} 2\,D_{ox} + H_2O$	
3	$v_o = V_o \cdot d_{red}$	$V_o = 1000$ *
	ATPase	
	$ADP_I + P_{i,I} + n_a H_E^+ \overset{v_a}{\rightleftharpoons} ATP_I + n_a H_I^+$	$n_a = 2$
4	$v_a = V_a\left(1 - \frac{[ATP]_I}{[ADP]_I \cdot [P_i]_I} \cdot \varphi_p \cdot 10^{n_a(\Delta\mu - \Delta\mu_a)/Z}\right)$	$V_a = 10$ * $\Delta\mu_a = -150$ mV
5	$\varphi_p = f_p + (1 - f_p) \cdot 10^{\Delta pH}$	$f_p = 0.2$
6	$\Delta pH = -f_\mu \cdot \Delta\mu/Z$	$f_\mu = 0.1$

electrochemical gradient which is equivalent to the gap of the midpoint potentials of the compounds A and D (cf. Appendix 1). The value was estimated from the data of NAD and cytochrome a_3 *.

For the rate law of the ATPase (Eqn. 4), the rapid equilibrium approximation is used again. The results of titration with inhibitors [10] indicate that the ATPase activity indeed exceeds the overall capacity of oxidative phosphorylation. The value used for the maximum velocity corresponds to a 3-fold capacity (note $P/O = 3$). As shown in Results, such a value is sufficient to fulfil the near-equilibrium condition used in the derivation of the rate law. The numbers of protons n_r and n_a, translocated in reactions 2 and 4, together with the proton necessary for charge compensation of the electrogenic adenine nucleotide exchange, determine the P/O ratio (see below). The numbers listed in Table I result in the classical P/O (3 H^+ per coupling site, 2 H^+ per ATP synthe-

* $E_0' = -320$ mV [22] and +380 mV [23].

span of midpoint potentials of A and C and to the standard phosphorylation potential (cf. Appendix 1); f_p, mole fraction of monovalent phosphate in the extramitochondrial compartment (cf. Appendix 2); f_μ, osmotic fraction of the proton electrochemical gradient; f_ψ, fraction of the membrane potential causing the asymmetry of the adenine nucleotide translocator in respect to the binding of ADP and of ATP (cf. Appendix 3); φ_p, ratio of mole fractions of monovalent phosphate on both sides of the membrane (cf. Appendix 2); subscripts I, E, intra- and extramitochondrial compartment, respectively.

No.	Equations	Parameters
	Translocation of phosphate	
	$P_{i,E}^{2-} + 2\ H_E^+ \rightleftharpoons P_{i,I}^{2-} + 2\ H_I^+$	
7	$[P_i]_I = [P_i]_E \cdot \varphi_p \cdot 10^{\Delta pH}$	
	Translocation of adenine nucleotides	
	$ADP_E + ATP_I \overset{v_t}{\rightleftharpoons} ADP_I + ATP_E$	
8	$v_t = V_t \dfrac{1 - \dfrac{[ATP]_E}{[ADP]_E} \cdot \dfrac{[ADP]_I}{[ATP]_I} \cdot 10^{\Delta\psi/Z}}{\left(1 + \dfrac{[ATP]_E}{[ADP]_E} \cdot 10^{f_\psi \Delta\psi/Z}\right) \cdot \left(1 + \dfrac{[ADP]_I}{[ATP]_I} \cdot 10^{(1-f_\psi)\,\Delta\psi/Z}\right)}$	$V_t = 4$ * $f_\psi = 0.6$
9	$\Delta\psi = \Delta\mu + Z \cdot \Delta pH$	
	Proton leak	
	$H_E^+ \overset{v_l}{\rightarrow} H_I^+$	
10	$v_l = V_l \cdot 10^{-\Delta\mu/Z}$	$V_l = 3 \cdot 10^{-4}$ *
	Steady-state relations	
	flux of electrons	
11	$v_r = v_h = v_o = v_{resp}$	
	flux of charges through the membrane	
12	$n_r \cdot v_r = n_a \cdot v_a + v_t + v_l$	
	flux of adenine nucleotides	
13	$v_a = v_t = v_{phos}$	

* Arbitrary units.

sized, 1 H^+ for the transport). The parameter $\Delta\mu_a$ is equivalent to the standard phosphorylation potential; it is shown in Appendix 1 that the notation of Eqn. 4 is simpler in this form. The value $\Delta\mu_a = -150$ mV was obtained from the standard phosphorylation potential estimated for the conditions in liver cytosol [24] *. Since the intramitochondrial pH deviates from the extramitochondrial conditions, this effect is corrected by the factor φ_p, as outlined in Appendix 2. According to Eqn. 5, φ_p can be computed from ΔpH and the mole fraction of monovalent phosphate **. ΔpH is a function of the total proton gradient $\Delta\mu$. Its portion depends on many conditions, in particular on the

* $\Delta G^{\circ\prime} = 29$ kJ/mol, cf. Ref. 25.

** Estimated from pH = 7.5 and $pK' = 6.8$ of monovalent phosphate [26].

ion composition of the medium [15,16]. Here, it was assumed that ΔpH is proportional to $\Delta\mu$ (Eqn. 6). The proportionality factor f_μ was selected so that ΔpH = 0.3 for $\Delta\mu$ = —200 mV.

The translocation of phosphate is very fast [27] so that the phosphate distribution is considered here to be in equilibrium under all conditions (Eqn. 7, for derivation see Appendix 2).

The adenine nucleotide translocator requires a more detailed rate law, since its maximum activity was found in the same order of magnitude as the overall rate of oxidative phosphorylation [28]. This is reflected by the value of the maximum rate given in Table I, for P/O = 3 it corresponds to 4/3 of the maximum rate of ATP production. Eqn. 8 is derived for a gated-pore mechanism [29,30], assuming saturation by ADP and/or ATP of the translocator on both sides of the membrane (see Appendix 3). The equation is in agreement with the effects of the membrane potential, as well as on the distribution equilibrium of adenine nucleotides [31] and on the Michaelis constant of external ATP [32]. The latter is expressed by the fraction f_ψ of the membrane potential; the value in Table I is estimated from experimental data (see Appendix 3). It is predicted by Eqn. 8 that an additional effect of the membrane potential exists on the inner side: the fraction $(1 - f_\psi)$ suppresses the binding of ADP in favour of ATP. Recent results of Krämer and Klingenberg [33] are in line with this.

The proton leak (Eqn. 10) represents the passive back-flow of protons through the coupling membrane. As in the other rate laws, exponential dependence on the driving proton electrochemical gradient is assumed. It causes a dependence of the proton conductivity on the proton gradient, which was experimentally observed, as well (e.g. Ref. 15). The selected value of the maximum velocity leads to a respiration rate in the resting state which is 10% of the maximum.

The remaining equations (Eqns. 11—13) describe the relationships between the rates of the several processes in the steady-state. All rates can be expressed by the rates of respiration and of phosphorylation. The latter are connected with each other because the sum of all charge fluxes through the membrane must be zero (Eqn. 12). Besides the electrogenic movements of protons caused by the respiratory chain, by the ATPase and by the proton leak, this includes the electrogenic ADP-ATP exchange. Eqn. 12 states that at a given rate of respiration, the rate of phosphorylation must be higher if ATP is utilized within mitochondria so that no net exchange of ADP and ATP proceeds. This was indeed recently demonstrated by Duszynski et al. [34].

Results and Discussion

Resting and active state of oxidative phosphorylation

The data predicted by the model for the resting and the active state of oxidative phosphorylation are compared in Table II with experimental observations. Since it was observed in experiments with isolated mitochondria that the respiration in the resting state can be inhibited to about half by blocking the ATPase or the adenine nucleotide translocator [3], some turnover of extramitochondrial ATP must be assumed in the experimental resting state. Presumably, it is caused by ATPase activities present as impurities in mitochon-

TABLE II

COMPARISON OF COMPUTED AND OBSERVED DATA

The computed data were obtained from the equations and parameter values presented in Table I assuming 10 mM P_i in the extramitochondrial compartment (for the procedure of computation see Appendix 4). The definition of 'theoretical' and 'experimental' resting state is given in the text. Observed data given without references are estimated as typical for rat liver mitochondria.

Quantity	Unit	Computed data			Observed data		
		'Theoretical' resting state	'Experimental' resting state	Active state	Resting state	Active state	Refs.
v_{resp}	per cent *	10.3	20.0	94.4	10 — 20	90 —100	
v_{phos}	per cent *	0.0	35.5	272	0.0	260 —300	
$[A_{red}]$	per cent	89.7	80.0	5.6	—	—	
$[C_{red}]$	per cent	0.01	0.02	0.09	—	—	
$-\Delta\mu$	mV	209	203	182	180 —230	170 —190	13—17 **
$-\Delta\psi$	mV	188	183	164	170 —200	150 —160	15, 16 **
ΔpH		0.35	0.34	0.30	0.3— 0.5	0.3— 0.5	15, 16 **
$[P_i]_I$	mM	44.4	42.6	36.4	38	36	5
$[ATP]_I/[ADP]_I$		2.14	1.26	0.172	2,8— 5	1.0	2, 35—37 **
$[ATP]_E/[ADP]_E$		2960	435	0.0	100 —400	<5	3, 36

* Referred to the maximum rate of respiration, as of uncoupled mitochondria.

** Also Küster, U., Letko, G., Kunz, W., Duszynski, J., Bogucka, K. and Wojtczak, L., personal communication.

drial preparations. Therefore, data were computed for a 'theoretical' resting state (rate of phosphorylation = zero) and for an 'experimental' resting state (assuming that the extramitochondrial ATP turnover increases the respiration rate up to 20% of its maximum).

Good accordance exists for the rates of respiration and of phosphorylation, for the proton electrochemical gradient and its electrical and osmotic components and for the intramitochondrial concentration of phosphate. The computed ATP/ADP ratios deviate to some extent from the observed data. The computed intramitochondrial ratios are lower, the extramitochondrial ratios are higher. But the deviations are not too wide, if the approximations made in the derivation of the model are considered. (For example, the effects of Mg^{2+} on the phosphorylation potential [25] and on the kinetics of adenine nucleotide translocation [28] are neglected.) No direct comparison of the computed reduction degrees is possible. Compound A (cf. reaction 1 in Table I) is defined as an hydrogen acceptor in the rate-limiting step of hydrogen supply. According to observations of Davis and Blair [38], this step must be localized between the substrate and NAD. They found that in the active state, the rate of hydrogen transfer between substrate and NAD becomes independent of the NAD/NADH ratio. The compound D is defined as the electron donator of the irreversible reaction step in the cytochrome oxidase mechanism. Possibly, this is a complex of several compounds [39].

The fit of the computed data to the experimental ones depends on the parameter values used in computation. The most critical parameters are: the maximum capacity, V_o, of the terminal oxidation step, which determines the part of energy transformed into the proton gradient (see Methodology), and the numbers of protons translocated by the respiratory chain (n_r) and by the ATP-ase (n_a). The proton stoichiometry also decides the height of the proton gradient, in which the energy transformed by the respiratory chain is stored, and the relationships between the proton gradient and the intra- and extramitochondrial phosphorylation potentials and, therefore, the resulting ATP/ADP ratios.

Relationships between energy fluxes and energy levels

The resting state and the active state are only limit states of the activity of oxidative phosphorylation [3]. Respiration rates computed between these limits versus the energy levels of different energy pools, are plotted in Fig. 2. The energy quantities are so selected that a direct comparison is possible between them. Per mole ATP delivered by mitochondria into the extramitochondrial space n_a protons are required for the synthesis of ATP and one additional proton is necessary to compensate both the electrogenic ATP-ADP exchange and the electroneutral movement of phosphate. (The electrogenic extrusion of this additional proton by the respiratory chain compensates the charge transfer of the adenine nucleotide exchange; the proton enters the mitochondria together with phosphate.) Therefore, the energy which must be delivered by the respiratory chain is $-(n_a + 1)F\Delta\mu$ per mol extramitochondrial ATP. After synthesis of ATP, the energy supply for erection of the extramitochondrial phosphorylation potential $\Delta G_{P,E}$ is given by the intramitochondrial phosphorylation potential $\Delta G_{P,I}$ plus the energy costs of the transport steps, which are $-F\Delta\mu$. The differences between these three energy quantities are wastes of

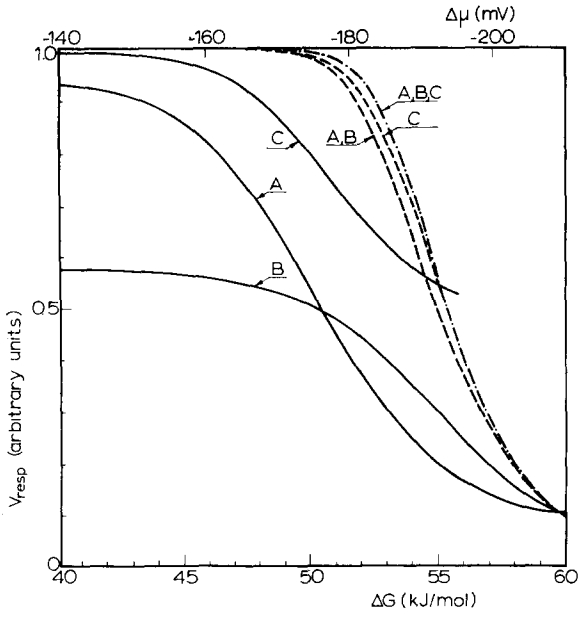

Fig. 2. Respiration rate as function of energy levels. Respiration rates and energy levels were computed for three conditions: (A) as in Table II; (B) concentration of extramitochondrial phosphate decreased by factor 10 ($[P_i]_E$ = 1 mM); (C) proton leak increased by factor 10 ($V_1 = 3.10^{-3}$). For each condition, the respiration rate was plotted vs the extramitochondrial phosphorylation potential ($\Delta G_{P,E}$, ———), vs. the intramitochondrial phosphorylation potential plus the energy put in by translocation of adenine nucleotides and of phosphate ($\Delta G_{P,I} - F\Delta\mu$, — — —), and vs the energy delivered by the respiratory chain for erection of the extramitochondrial phosphorylation potential ($-(n_a + 1)F\Delta\mu$, · — · — ·). For comparison, the energy levels are also expressed as equivalent proton electrochemical gradient in the scale at the top.

energy which are necessary to drive the synthesis of ATP and its exchange for ADP. (If the phosphate distribution is near to equilibrium, as considered here, the energy waste by the translocation of phosphate is negligible.)

In Fig. 2, the respiration rates are given for three different conditions: the same as in Table II, decreased concentration of extramitochondrial phosphate and increased passive back-flow of protons. The dependence of the respiration rate on the proton electrochemical gradient is the same in all three cases. Since the decrease of the proton gradient is the signal for the activation of the electron flux through the respiratory chain, such behaviour must be expected. It decreases the potential gap between the redox carriers on the substrate and oxygen side of the respiratory chain. The substrate side becomes more oxidized and so the input of hydrogen increases. The oxygen side becomes more reduced, it accelerates the reduction of oxygen. The slope of the curve in Fig. 2 demonstrates the high sensitivity of the respiration rate to changes in the proton gradient (cf. the scale in mV at the top of the figure). This high apparent cooperativity is caused by the stoicheiometric structure; small changes in the proton gradient are amplified by the large total number of protons translocated per two electrons. Experimental results recently obtained by Küster et al. (Küster, U., Letko, G., Kunz, W., Duszynski, J., Bogucka, K. and Wojtczak, L., personal communication) show that such uniform dependence on the proton gradient exists in a wide range of the respiration rate, whether the respiration

is stimulated by phosphorylation of exogeneous ADP or by uncoupling.

In the 'theoretical' resting state, the proton gradient must be in equilibrium with the phosphorylation potentials within and outside mitochondria. The different lines in Fig. 2 cross at this point. The crossing point is shifted to higher rates of respiration and lower energy potentials by raised nonphosphorylating proton fluxes (e.g. in partially uncoupled mitochondria). The experimental investigation of the extramitochondrial phosphorylation potential in the resting state revealed that it becomes decreased by phosphate [36]. Considering some turnover of ATP in the 'experimental' resting state [3], the results shown in Fig. 2 are in complete agreement with this observation.

If the energy levels are lower than in the 'theoretical' resting state, net synthesis of ATP and its exchange for extramitochondrial ADP proceed. Then the curves deviate more and more with increasing fluxes indicating the energy wastes necessary to drive the synthesis of ATP and the adenine nucleotide exchange. The results of Küster et al. (Küster, U., Letko, G., Kunz, W., Duszynski, J., Bogucka, K. and Wojtczak, L., personal communication) demonstrate that the energy waste by the ATPase is very small indeed, so it justifies the approximations made here for the rate law of this reaction.

The energy waste due to the adenine nucleotide exchange is much larger and different in the three cases considered, therefore, no uniform dependence of the respiration rate on the extramitochondrial phosphorylation potential exists. The effect of phosphate predicted by the model is in accordance with the experimental observations [4—6]. If the concentration of extramitochondrial phosphate is considerably below 10 mM, the maximum rate of oxidative phosphorylation is not reached. This is caused by a competitive inhibition of the adenine nucleotide translocator due to the low intramitochondrial ATP/ADP ratio under such a condition. (As indicated in Fig. 2, phosphate has no effect on the intramitochondrial phosphorylation potential, so that for constant rates of respiration, the intramitochondrial ATP/ADP ratio falls in proportion to the concentration of phosphate.) At rates of oxidative phosphorylation considerably lower than the maximum, the energy waste by the adenine nucleotide translocator increases with the concentration of phosphate. Again, the effect is caused by a competitive inhibition of the translocator, but in this case by extramitochondrial ATP. (If constant extramitochondrial phosphorylation potentials are considered, the ATP/ADP ratio grows with the concentration of phosphate.) This is the reason for the nearly phosphate-independent control of respiration by the ATP/ADP ratio observed in earlier experiments [4—6].

The curves shown in Fig. 2 demonstrate a further phenomenon. If respiration is activated by processes other than phosphorylation of exogenous ADP, the divergence between the extramitochondrial phosphorylation potential and the proton gradient disappears. Therefore, the resulting phosphorylation potential is higher than that of phosphorylation of exogenous ADP at the same rate of respiration. Such behaviour was already observed with liver mitochondria utilizing intramitochondrial ATP in citrulline synthesis [40].

Finally, from the results presented in Fig. 2, it follows that the relationships between fluxes and forces are neither linear nor constant, as generally assumed in attempts to interpret effects of metabolic control by concepts of irrever-

sible thermodynamics (e.g. Ref. 41—44). For instance, the effects of phosphate on the control of oxidative phosphorylation result in different driving forces for the same flux through the adenine nucleotide translocator. The reason lies in the extent of kinetic inhibition of the adenine nucleotide translocation by extramitochondrial ATP and intramitochondrial ADP. If the inhibition increases, the same flux requires a higher driving force to overcome the 'resistance'. More generally expressed, the biocatalyzers are sensitive not only to changes in the driving force but also to influences upon their capacity produced by inhibitors or activators.

Acknowledgement

The author wishes to thank Prof. Kunz for his steady interest in this work, and Dr. Letko and Dr. Küster for many stimulating discussions.

Appendix 1

Approximate rate law of near-equilibrium reactions

The net flux of a reversible reaction is the difference of two opposite fluxes

$$v = \vec{v} - \overleftarrow{v} \tag{1}$$

Both $\vec{v}$ and $\overleftarrow{v}$ are functions of the composition of the reaction system. It will be shown that in near-equilibrium, the net flux is more sensitive to changes in the $\overleftarrow{v}/\vec{v}$ ratio than to changes in $\vec{v}$ or $\overleftarrow{v}$.

From Eqn. 1 it follows,

$$v = \vec{v}(1 - \overleftarrow{v}/\vec{v}) \tag{2}$$

and for any change dv

$$dv = (1 - \overleftarrow{v}/\vec{v})\, d\vec{v} - \vec{v}d(\overleftarrow{v}/\vec{v}) \tag{3}$$

As the reaction approaches the equilibrium ($\overleftarrow{v}/\vec{v} = 1$), the factor $(1 - \overleftarrow{v}/\vec{v})$ decreases, so that changes in $\vec{v}$ become negligible in comparison with those in $\overleftarrow{v}/\vec{v}$. Then $\vec{v}$ in Eqn. 2 can be considered as a constant,

$$\vec{v} = V_{app}, \tag{4}$$

which may be interpreted as the apparent maximum velocity or capacity of the reaction.

The flux ratio $\overleftarrow{v}/\vec{v}$ is determined by the affinity A ($A = -\Delta G$) of the reaction it follows (e.g. Ref. 45)

$$v = V_{app}(1 - e^{-A/RT}) \tag{5}$$

For a chemical reaction $e^{-A/RT} = \Gamma/K$, where Γ is the actual mass-action ratio and K the equilibrium constant. So, the rate law can be approximated as

$$v = V_{app}(1 - \Gamma/K) \tag{6}$$

If the chemical reaction is coupled with the translocation of n protons against an electrochemical gradient $\Delta\mu$,

$$A = n \cdot F \cdot \Delta\mu - (\Delta G^\circ + RT \ln \Gamma) \tag{7}$$

ΔG° is the standard free energy change of the chemical reaction (not coupled to proton translocation). Eqn. 7 is easier to handle if ΔG° is replaced by an equivalent proton electrochemical gradient

$$\Delta\mu_o = \frac{\Delta G^\circ}{n \cdot F} \tag{8}$$

and this finally results in

$$v = V_{app}(1 - \Gamma \cdot 10^{-n(\Delta\mu - \Delta\mu_o)/Z}) \tag{9}$$

For redox reactions, the value $\Delta\mu_o$ can be obtained, too, from the span, ΔE_o, of midpoint potentials and the number, m, of electrons exchanged in the redox process

$$\Delta\mu_o = \frac{m}{n} \Delta E_o \,. \tag{10}$$

Appendix 2

pH effects on equilibrium caused by phosphate ions

The ionic state of phosphate depends on the actual pH. Since equilibrium constants are usually referred to the total concentration instead of the particular ionic species taking part in the reactions, they are functions of pH. It is possible to express this pH effect by means of a factor φ_p, which relates the fraction of monovalent phosphate $[P_i^-]/[P_i]$ at a given reference value of pH′ to that at an actual pH value:

$$\varphi_p = \frac{([P_i^-]/[P_i])_{pH'}}{([P_i^-]/[P_i])_{pH}} \,. \tag{11}$$

In this way, the effect of pH on the equilibrium constant of ATP formation can be approximated by the factor φ_p, if the reaction

$$ADP + P_i^- \rightleftharpoons ATP \tag{12}$$

is considered to be independent of pH. (This is admitted, since the ionization constants of ATP^{3-} and ADP^{2-} are not quite different, cf. Ref. 46).

Then, the quotient $[ATP]/([ADP] \cdot [P_i^-])$ is not influenced by pH, so that for any pH value, the mass action quotient $[ATP]/([ADP] \cdot [P_i])$ can be referred to its value K' at pH′ as

$$\frac{[ATP]}{[ADP] \cdot [P_i]} \cdot \varphi_p = K' \tag{13}$$

Similarly, the electroneutral distribution of phosphate between two compartments with pH and pH′ may be described by φ_p. From the distribution equilibrium of monovalent phosphate

$$[P_i^-]_{pH} = [P_i^-]_{pH'} \cdot 10^{\Delta pH} \tag{14}$$

with $\Delta pH = pH - pH'$ results for total phosphate

$$[P_i]_{pH} = [P_i]_{pH'} \cdot \varphi_p \cdot 10^{\Delta pH} \tag{15}$$

The factor φ_p can be expressed as function of ΔpH. Since, only monovalent and divalent phosphate must be considered in the physiological region of pH, it follows from the ionization equilibrium

$$\left(\frac{[P_i^-]}{[P_i]}\right)_{pH} = \frac{1}{1 + 10^{pH-pK}} \tag{16}$$

When the corresponding expression at pH′ is denoted by f_p and the relation pH = pH′ + ΔpH is used, Eqn. 11 leads to

$$\varphi_p = f_p + (1 - f_p)\, 10^{\Delta pH} . \tag{17}$$

Appendix 3

Rate law of the adenine nucleotide translocator

Formally, the gated-pore mechanism discussed for the adenine nucleotide translocator [29,30] is equivalent to a ping-pong enzyme reaction. The necessary information about the corresponding complete rate equation is given by Cleland [47]. The denominator contains eight different terms but can be considerably simplified, since in general, the concentrations of ATP and ADP are high in comparison to their Michaelis constants. Then, only those terms which include products of two concentrations are important (as $[ADP]_E \cdot [ATP]_I$, etc.). Using Cleland's notation, it follows for the rate of $ADP_E - ATP_I$ exchange

$$v = \frac{V_1\left([ADP]_E \cdot [ATP]_I - \frac{1}{K_{eq}}[ATP]_E \cdot [ADP]_I\right)}{[ADP]_E \cdot [ATP]_I + \frac{K_d}{K_{it}}[ATP]_E \cdot [ATP]_I + \frac{K_{t'}}{K_{id'}}[ADP]_E \cdot [ADP]_I + \frac{K_d}{K_{it}} \cdot \frac{K_{it'}}{K_{d'}}[ATP]_E \cdot [ADP]_I} \tag{18}$$

The kinetic constants occurring in the denominator are Michaelis constants (without the subscript i) and inhibition constants (with the subscript i), the subscripts d, t, d′ and t′ stand for ADP_E, ATP_E, ADP_I and ATP_I. Eqn. 18 can be rearranged so that only ATP/ADP ratios occur

$$v = \frac{V_1\left(1 - \frac{1}{K_{eq}} \cdot \frac{[ATP]_E}{[ADP]_E} \cdot \frac{[ADP]_I}{[ATP]_I}\right)}{1 + \frac{K_d}{K_{it}} \cdot \frac{[ATP]_E}{[ADP]_E}\left(1 + \frac{K_{it'}}{K_{d'}} \cdot \frac{[ADP]_I}{[ATP]_I}\right) + \frac{K_{t'}}{K_{id'}} \cdot \frac{[ADP]_I}{[ATP]_I}} \tag{19}$$

According to experimental investigations [31], the equilibrium constant is given by

$$K_{eq} = 10^{-\Delta\psi/Z} \tag{20}$$

The quotient K_d/K_{it} can be estimated from the data reported by Souverijn et al. [32]. The Michaelis constant of ADP was found to be 1—2 μM, independent of the energy state of mitochondria, whereas, the inhibition constant of

ATP was about 150 μM in energized mitochondria and approached the Michaelis constant of ADP in uncoupled mitochondria. Such behaviour is expressed by the equation

$$\frac{K_d}{K_{it}} = 10^{f_\psi \Delta\psi/Z} \tag{21}$$

where f_ψ denotes the fraction of the membrane potential which causes the decreased affinity to ATP. Assuming $\Delta\psi = -180$ mV in energized mitochondria, $f_\psi \approx 0.6$.

The remaining quotients of kinetic constants can be estimated by means of the Haldane equations [47]

$$K_{eq} = \frac{V_1}{V_2} \cdot \frac{K_{id'}}{K_{id}} \cdot \frac{K_t}{K_{t'}} = \frac{V_1}{V_2} \cdot \frac{K_{d'}}{K_d} \cdot \frac{K_{it}}{K_{it'}} \tag{22}$$

Supposing identical maximum velocities, V_1 and V_2 of the forward and the reversed reactions (equal maximum velocities for exchange of external ADP and ATP were found [32]) it follows with Eqns. 20 and 21

$$\frac{K_{it'}}{K_{d'}} = 10^{(1-f_\psi)\Delta\psi/Z} \tag{23}$$

If the Michaelis constants and the inhibition constants are considered to be equal (as it is the case for ATP [32]), the following relation exists

$$\frac{K_{t'}}{K_{id'}} = \frac{K_{it'}}{K_{d'}} \tag{24}$$

With Eqns. 20, 21, 23 and 24, the rate law finally gets the form

$$v = \frac{V_1\left(1 - \frac{[ATP]_E}{[ADP]_E} \cdot \frac{[ADP]_I}{[ATP]_I} \cdot 10^{\Delta\psi/Z}\right)}{\left(1 + \frac{[ATP]_E}{[ADP]_E} \cdot 10^{f_\psi \Delta\psi/Z}\right)\left(1 + \frac{[ADP]_I}{[ATP]_I} \cdot 10^{(1-f_\psi)\Delta\psi/Z}\right)} \tag{25}$$

Appendix 4

Performance of computations

The set of equations listed in Table I describes steady states of oxidative phosphorylation. The equations were so transformed that with the aid of a computer all variables could be calculated as function of v_{resp}: from Eqns. 1 and 11 (the numbers refer to Table I),

$$a_{ox} = \frac{v_{resp}}{V_h}\ ; \tag{26}$$

from Eqns. 3 and 11,

$$d_{red} = \frac{v_{resp}}{V_o}\ ; \tag{27}$$

from Eqns. 2 and 11,

$$\Delta\mu = \Delta\mu_r - \frac{Z}{n_r}\log\left(1 - \frac{v_{resp}}{V_r}\right)\left(\frac{1-a_{ox}}{a_{ox}}\right)\left(\frac{1-d_{red}}{d_{red}}\right)^2 ; \tag{28}$$

from Eqns. 5, 6, 7, 9 and 10,

ΔpH, φ_p, $[P_i]_I$, $\Delta\psi$ and v_l, respectively;

from Eqns. 11—13,

$$v_{phos} = \frac{n_r v_{resp} - v_l}{n_a + 1} ; \tag{29}$$

from Eqns. 4 and 13,

$$\frac{[ATP]_I}{[ADP]_I} = \frac{(1 - v_{phos}/V_a)[P_i]_I}{\varphi_P \cdot 10^{n_a(\Delta\mu - \Delta\mu_a)/Z}} ; \tag{30}$$

from Eqns. 8 and 13,

$$\frac{[ATP]_E}{[ADP]_E} = \frac{1 - \frac{v_{phos}}{V_t}\left(1 + \frac{[ADP]_I}{[ATP]_I}\, 10^{(1-f_\psi)\Delta\psi/Z}\right)}{\left(1 + \frac{v_{phos}}{V_t}\right)\cdot\frac{[ADP]_I}{[ATP]_I}\, 10^{\Delta\psi/Z} + \frac{v_{phos}}{V_t}\, 10^{f_\psi\Delta\psi/Z}} \tag{31}$$

The values $\Delta G_{P,E}$, $\Delta G_{P,I}$ and F used for construction of Fig. 2 were calculated from the equations

$$\Delta G_{P,E} = 2.3RT\left(\log\frac{[ATP]_E}{[ADP]_E \cdot [P_i]_E} - \frac{n_a + 1}{Z}\Delta\mu_a\right) , \tag{32}$$

$$\Delta G_{P,I} = 2.3RT\left(\log\frac{[ATP]_I}{[ADP]_I \cdot [P_i]_I}\cdot\varphi_p - \frac{n_a}{Z}\Delta\mu_a\right) , \tag{33}$$

$$F = \frac{2.3RT}{Z} , \tag{34}$$

$$2.3RT = 5.7 \text{ kJ/mol} . \tag{35}$$

The computed data listed in Table II for the active and 'theoretical' resting state were obtained by an iterative procedure searching the solutions $[ATP]_E/[ADP]_E = 0$ and $v_{phos} = 0$, respectively.

References

1 Küster, U., Bohnensack, R. and Kunz, W. (1973) in Carbohydrate Metabolism in Animal Tissues and its Regulation, Abstr. 2nd Joint Symposium of the All-Union Biochemical Society of U.S.S.R. and the Biochemical Society of G.D.R., pp. 48—49, Nauka, Moscow

2 Davis, E.J. and Lumeng, L. (1975) J. Biol. Chem. 250, 2275—2282

3 Küster, U., Bohnensack, R. and Kunz, W. (1976) Biochim. Biophys. Acta 440, 391—402

4 Kunz, W., Bohnensack, R., Böhme, G., Küster, U., Letko, G. and Schönfeld, P. (1981) Arch. Biochem. Biophys., submitted

5 Böhme, G., Hartung, K.J. and Kunz, W. (1978) in Bioenergetics at Mitochondrial and Cellular Levels (Wojtczak, L., Lenartowicz, E. and Zborowski, J., eds.), pp. 79—102, Nencki Institute of Experimental Biology, Warsaw

6 Davis, E.J. and Davis-van Thienen, W.I.A. (1978) Biochem. Biophys. Res. Commun. 83, 1260—1266
7 Boyer, P.D., Chance, B., Ernster, L., Mitchell, P., Racker, E. and Slater, E.C. (1977) Ann. Rev. Biochem. 46, 955—1026
8 Bohnensack, R. and Kunz, W. (1978) Acta Biol. Med. Germ. 37, 97—112
9 Bienfait, H.F., Jacobs, J.M.C. and Slater, E.C. (1975) Biochim. Biophys. Acta 376, 446—457
10 Küster, U. (1976) Thesis, Technische Hochschule, Magdeburg
11 Wilson, D.F., Erecinska, M., Owen, C.S. and Mela, L. (1974) in Dynamics of Energy-transducing Membranes (Ernster, L., Estabrook, R.W. and Slater, E.C., eds.), pp. 221—231, Elsevier, Amsterdam
12 Erecinska, M., Veech, R.L. and Wilson, D.F. (1974) Arch. Biochem. Biophys. 160, 412—421
13 Van Dam, K., Wiechmann, A.H.C.A. and Hellingwerf, K.J. (1977) Biochem. Soc. Trans. 5, 485—487
14 Azzone, G.F., Pozzan, T. and Massari, S. (1978) Biochim. Biophys. Acta 501, 307—316
15 Nicholls, D.G. (1974) Eur. J. Biochem. 50, 305—315
16 Azzone, G.F., Bragadin, M., Pozzan, T. and Dell'Antone, P. (1976) Biochim. Biophys. Acta 459, 96—109
17 Azzone, G.F., Pozzan, T., Massari, S. and Bragadin, M. (1978) Biochim. Biophys. Acta 501, 296—306
18 Brand, M.D., Harper, W.G., Nicholls, D.G. and Ingledew, W.J. (1978) FEBS Lett. 95, 125—129
19 Hinkle, P.C. and Yu, M.L. (1979) J. Biol. Chem. 254, 2450—2455
20 Alexandre, A. and Lehninger, A.L. (1979) J. Biol. Chem. 254, 11 555—11 560
21 Azzone, G.F., Pozzan, T., Bragadin, M. and Miconi, V. (1979) J. Biol. Chem. 254, 10 218—10 219
22 Burton, K. and Wilson, T.H. (1953) Biochem. J. 54, 86—94
23 Wilson, D.F., Lindsay, J.G. and Brocklehurst, E.S. (1972) Biochim. Biophys. Acta 256, 277—286
24 Akerboom, T.P.M., Bookelman, H., Zuurendonk, P.F., van der Meer, R. and Tager, J.M. (1978) Eur J. Biochem. 84, 413—420
25 Rosing, J. and Slater, E.C. (1972) Biochim. Biophys. Acta 267, 275—290
26 Rauen, H.M. (1964) Biochemisches Taschenbuch, 2nd edn., Vol. 2, p. 49, Springer, Berlin
27 Coty, W.A. and Pedersen, P.L. (1975) Mol. Cell. Biochem. 9, 109—124
28 Pfaff, E., Heldt, H.W. and Klingenberg, M. (1969) Eur. J. Biochem. 10, 484—493
29 Vignais, P.V. (1976) Biochim. Biophys. Acta 456, 1—38
30 Klingenberg, M. (1979) Trends Biochem. Sci. 4, 249—252
31 Klingenberg, M. and Rottenberg, H. (1977) Eur. J. Biochem. 73, 125—130
32 Souverijn, J.H.M., Huisman, L.A., Rosing, J. and Kemp, A., Jr. (1973) Biochim. Biophys. Acta 305 185—198
33 Krämer, R. and Klingenberg, M. (1979) in Function and Molecular Aspects of Biomembrane Transport (Quagliariello, E., Palmieri, F., Papa, S. and Klingenberg, M., eds.), pp. 515—518, Elsevier/North Holland, Amsterdam
34 Duszynski, J., Bogucka, K., Letko, H.G., Küster, U. and Wojtczak, L. (1979) in Function and Molecular Aspects of Biomembrane Transport (Quagliariello, E., Palmieri, F., Papa, S. and Klingenberg, M. eds.), pp. 309—312, Elsevier/North-Holland, Amsterdam
35 Heldt, H.W., Klingenberg, M. and Milovancev, M. (1972) Eur. J. Biochem. 30, 434—440
36 Slater, E.C., Rosing, J. and Mol. A. (1973) Biochim. Biophys. Acta 292, 534—553
37 Letko, G., Küster, U., Duszynski, J. and Kunz, W. (1980) Biochim. Biophys. Acta, 593, 196—203
38 Davis, E.J. and Blair, P.V. (1977) Biochem. Biophys. Res. Commun. 77, 1017—1023
39 Wilson, D.F., Owen, C.S. and Holian, A. (1977) Arch. Biochem. Biophys. 182, 749—762
40 Letko, G. and Küster, U. (1979) Acta Biol. Med. Germ. 38, 1379—1385
41 Van der Meer, R., Akerboom, T.P.M., Groen, A.K. and Tager, J.M. (1978) Eur. J. Biochem. 84, 421—428
42 Stucki, J.W. (1978) in Energy Conservation in Biological Membranes (Schäfer, G. and Klingenberg M., eds.), pp. 264—287, Springer, Berlin
43 Rottenberg, H. (1979) Biochim. Biophys. Acta 549, 225—253
44 Westerhoff, H.V. and van Dam, K. (1979) Curr. Topics Bioenerg. 9, 1—62
45 Glansdorff, P. and Prigogine, I. (1971) Thermodynamic Theory of Structure, Stability and Fluctuations, Wiley-Interscience, London
46 Phillips, R.C., George, P. and Rutman, R.J. (1966) J. Am. Chem. Soc. 88, 2631—2640
47 Cleland, W.W. (1963) Biochim. Biophys. Acta 67, 104—137